Inorg. Chem. **2008**, *47*, 592–601

Ag(I)-Based Tectons for the Construction of Helical and *meso*-Helical Hydrogen-Bonded Coordination Networks

David A McMorran*

Department of Chemistry, University of Otago, P.O. Box 56, Dunedin, New Zealand

Received September 28, 2007

The new ligand 4-(3-(2-pyridyl)pyrazol-1-ylmethyl)benzoic acid (**L**) has been prepared and characterized. This bifunctional ligand incorporates both a chelating region, with two nitrogen donors, suitable for chelating to soft transition metal ions, and a self-complementary hydrogen-bonding region which can facilitate intermolecular association of ligands or ligand-based complexes. X-ray structural analysis of the ligand shows it to adopt a one-dimensional helical polymeric structure, with adjacent ligands hydrogen bonded to each other. Reaction of **L** with silver(I) salts (AgOTf (**1**, **1**·1.5H_2O), $AgNO_3$ (**2**), $AgPF_6$ (**3**·CH_3OH), and $AgClO_4$ (**4**·CH_3OH)) results in the formation of complexes with 2:1 stoichiometries. X-ray structural analysis of these complexes shows that, in each case, one-dimensional chain structures are obtained where chiral AgL_2 tectons are hydrogen bonded together, either directly or mediated by anions or solvent. Structures with either helical or *meso*-helical structures are observed.

Introduction

As interest in the field of metallosupramolecular chemistry continues to grow, so too has the range of strategies concerning how to deliberately incorporate transition metal ions into supramolecular systems. For much of its development, the concept of using transition metal ions as 'glue' to assemble suitable organic fragments into a whole has been a dominant theme in metallosupramolecular synthesis.[1] By taking advantage of the unique geometrical and electronic properties of certain transition metal ions, a vast array of structures with fascinating structural and functional properties has been reported.[2] An underlying paradigm in the construction of these systems is that they are formed by the self-assembly of suitable components, or tectons, (transition metal ions and ligands) and that the covalent bonds formed between the metal ion and the ligand donor atom(s) during the assembly process are labile enough that a self-correction of the assembly is possible. For this reason, some combinations of metal ion and donor atom, such as palladium(II) or silver(I) and pyridine nitrogen donors, have become very familiar in the literature. However, incorporation of less labile metal ions, such as ruthenium(II), present problems using this 'metal ions as glue' approach.

More recently a second theme has emerged, that of using noncovalent intermolecular interactions to assemble suitable transition metal ion containing fragments into a supramolecular structure. Such an approach overcomes the problems associated with nonlabile metal ion−ligand bonds by using the metal complex as a whole as the tecton for the assembly process. While various suitable intermolecular interactions might be imagined, in practice the one which has been most explored is hydrogen bonding.[3] The strength and, in particular, the directionality of hydrogen bonds make them an ideal way of rationally assembling supramolecular systems, as is clearly seen in biology and exemplified in the structure of DNA. In order to maximize these properties of hydrogen bonds, however, two factors must be considered, the relative orientations of the hydrogen bond donor(s) and acceptor(s) and also the numbers of donors and acceptors. With this in

* E-mail: davidm@chemistry.otago.ac.nz.

(1) (a) Steel, P. J. *Chem. N.Z.* **2003**, *67*, 57−60. (b) Holliday, B. J.; Mirkin, C. A. *Angew. Chem., Int. Ed.* **2001**, *40*, 2022−2043. (c) Swiegers, G. F.; Malefetse, T. J. *Chem. Rev.* **2000**, *100*, 3483−3537. (d) Baxter, P. N. W. In *Comprehensive Supramolecular Chemistry*; Atwood, J. L., Davies, J. E. D., MacNicol, D. D., Vögtle, F., Lehn, J.-M., Eds.; Pergammon Press: New York 1996; Vol. 9, pp 166−211.

(2) (a) Steel, P. J. *Acc. Chem. Res.* **2005**, *38*, 243−250. (b) Wurthner, F.; You, C. C.; Saha-Moller, C. R. *Chem. Soc. Rev.* **2004**, *33*, 133−146. (c) Janiak, C. *Dalton Trans.* **2003**, 2781−2804. (d) Siedel, S. R.; Stang, P. J. *Acc. Chem. Res.* **2002**, *35*, 972−983. (e) Dinolfo, P. H.; Hupp, J. T. *Chem. Mater.* **2001**, *13*, 3113−3125.

(3) For reviews of recent results, see (a) Braga, D.; Brammer, L.; Champness, N. R. *Cryst. Eng. Comm.* **2005**, *7*, 1−19. (b) Kitagawa, S.; Uemura, K. *Chem. Soc. Rev.* **2005**, *34*, 109−119. (c) Roesky, H. W.; Andruh, M. *Coord. Chem. Rev.* **2003**, *236*, 91−119. (d) Beatty, A. M. *Coord. Chem. Rev.* **2003**, *246*, 131−143. (e) Desiraju, G. R. *Acc. Chem. Res.* **2002**, *35*, 565−573. (f) Beatty, A. M. *CrystEngComm.* **2001**, *51*, 1−13. (g) Aakeröy, C. B.; Beatty, A. M. *Aust. J. Chem.* **2001**, *54*, 409−421.

10.1021/ic701919r CCC: $40.75
Published on Web 12/08/2007

mind, various reliable synthons, such as carboxylic acids, oximes, and amides have been explored in the area of organic crystal engineering.[4] Since the early elucidation of the concept,[5] a number of workers have reported the assembly of transition metal complex tectons in which such hydrogen-bonding synthons, remote from the metal binding site of the ligand, assemble either in self-complementary fashion or to other organic species to form infinite metallosupramolecular systems with various structures.[3] In particular, a number of reports of such systems using nicotinic acid and its derivatives have appeared.[6] It is noteworthy, however, that few of these explore ligands with chelating donor sites, thereby limiting some of the inherent geometrical information imparted by the transition metal ion, which can be lost due to the flexibility in orientation of the coordinated ligands.

While this new approach has led to the preparation of various types of metallosupramolecular systems, one particular type of structure, the helix, which has featured as a favorite target of metallosupramolecular chemistry since its inception,[7] has been relatively elusive. Helices are of interest because of their inherent chirality, and both discrete helicates and helical polymeric structures have received a great deal of attention.[8] In the 'metal ions as glue' approach, helices have been prepared by the wrapping of organic ligands with multiple metal binding sites around metal ions lying on a screw axis,[9] and much effort has been devoted to the development of such ligands.[10] In contrast, reports of helices assembled using hydrogen bonding are much less common.[11] One approach has been to use hydrogen bonding to assemble the organic ligands which wrap around the metal ions.[12] However, most of the reported examples appear to have resulted serendipitously from intermolecular OH···halogen[13] or CH···halogen[14] interactions. Instances where more reliable synthons have been deliberately employed are rare.

Scheme 1 Bifunctional Ligand, **L**, Showing the Orthogonal Binding Sites

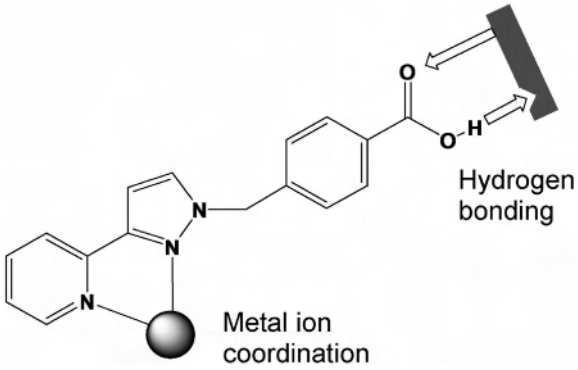

The current work reports the synthesis and characterization of the new bifunctional ligand 4-(3-(2-pyridyl)pyrazol-1-ylmethyl)benzoic acid, **L**, which has been designed with two orthogonal binding sites—a metal ion chelating site and a remote hydrogen-bonding surface (Scheme 1). Ligands based on the 2-pyridyl-pyrazole chelating system have been shown by us[15] and others[16] to both form stable metal complexes and to have high structural diversity due to the ready elaboration of the pyrazole ring by various organic fragments.

Reaction of this new ligand with silver(I) salts gives complexes with 2:1 ligand to metal ratios. As expected, the Ag(I) ions bind exclusively to the softer N donors, rather than the harder COOH donors which instead, in all cases, facilitate the formation of infinite one-dimensional polymeric structures by the assembly of Ag$\mathbf{L}_2$ tectons. Importantly,

(4) (a) Aakeröy, C. B.; Desper, J.; Scott, B. M. T. *Chem. Commun.* **2006**, 1445−1447. (b) Braga, D.; Maini, L.; Polito, M.; Greponi, F. *Struct. Bonding* **2004**, *111*, 1−32. (c) Burrows, A. D. *Struct. Bonding* **2004**, *108*, 55−96. (d) Fredericks, J. R.; Hamilton, A. D. In *Comprehensive Supramolecular Chemistry*; Atwood, J. L.; Davies, J. E. D.; MacNicol, D. D.; Vögtle, F.; Lehn, J.-M., Eds.; Pergammon Press: New York 1996; Vol. 9, pp 565−594. (e) Desiraju, G. R. *Angew. Chem., Int. Ed. Engl.* **1995**, *34*, 2311−2327.

(5) (a) Munakata, M.; Wu, L. P.; Yamamoto, M.; Kuroda-Sowa, T.; Maekawa, M. *J. Am. Chem. Soc.* **1996**, *118*, 3117−3124. (b) Burrows, A. D.; Chan, C.-W.; Chowdhry, M. M.; McGrady, J. E.; Mingos, D. M. P. *Chem. Soc. Rev.* **1995**, *24*, 329−339.

(6) (a) Aakeröy, C. B.; Beatty, A. M.; Leinin, D. S. *J. Am. Chem. Soc.* **1998**, *120*, 7383−7384. (b) Aakeröy, C. B.; Beatty, A. M. *Cryst. Eng.* **1998**, *1*, 39−49. (c) Aakeröy, C. B.; Beatty, A. M. *Chem. Commun.* **1998**, 1067−1068.

(7) (a) He, C.; Zhao, Y.; Guo, D.; Lin, Z.; Duan, C. *Eur. J. Inorg. Chem.* **2007**, 3451−3463. (b) Seeber, G.; Tiedemann, B. E. F.; Raymond, K. N. *Top. Curr. Chem.* **2006**, *265*, 147−183. (c) Albrecht, M. *Top. Curr. Chem.* **2005**, *248*, 105−139. (d) Piguet, C.; Borkovec, M.; Hamacek, J.; Zeckert, K. *Coord. Chem. Rev.* **2005**, *249*, 705−726. (e) Han, L.; Hong, M. *Inorg. Chem. Commun.* **2005**, *8*, 406−419. (f) Hannon, M. J.; Childs, L. J. *Supramol. Chem.* **2004**, *16*, 7- 22. (g) Albrecht, M. *Chem. Rev.* **2001**, *101*, 3457−3497. (h) Piguet,C.; Bernardinelli, G.; Hopfgartner, G. *Chem. Rev.* **1997**, *97*, 2005−2062. (i) Constable, E. C. In *Comprehensive Supramolecular Chemistry*; Atwood, J. L.; Davies, J. E. D.; MacNicol, D. D.; Vögtle, F.; Lehn, J.-M., Eds.; Pergammon Press: New York 1996; Vol. 9, pp 213−252.

(8) For some recent examples involving silver(I), see: (a) Lue, X.-Q.; Qiao, Y.-Q.; He, J.-R.; Pan, M.; Kang, B.-S.; Su, C.-Y. *Cryst. Growth Des.* **2006**, *6*, 1910−1914. (b) Beauchamp, D. A.; Loeb, S. J. *Supramol. Chem.* **2005**, *17*, 617−622. (c) Chen, X.-D.; Du, M.; Mak, T. C. W. *Chem. Commun.* **2005**, 4417−4419. (d) Valencia, L.; Bastida, R.; Macias, A.; Vicente, M.; Perez- Lourido, P. *New J. Chem.* **2005**, *29*, 424−426. (e) Kalra, M. K.; Zhang, H.; Son, D. Y. *Inorg. Chem. Commun.* **2004**, *7*, 1019−1022. (f) Schultheiss, N.; Powell, D. R.; Bosch, E. *Inorg. Chem.* **2003**, *42*, 8886−8890. (g) Kawano, T.; Du, C.-X.; Araki, T.; Ueda, I. *Inorg. Chem. Commun.* **2003**, *6*, 165−167. (h) Tuna, F.; Hamblin, J.; Clarkson, G.; Errington, W.; Alcock, N. W.; Hannon, M. J. *Chem.-Eur. J.* **2002**, *8*, 4957−4964. (i) Steel, P. J.; Sumby, C. J. *Inorg. Chem. Commun.* **2002**, *5*, 323−327. (j) Caradoc-Davies, P. L.; Hanton, L. R. *Chem. Commun.* **2001**, 1098−1099.

(9) Khatua, S.; Stoeckli-Evans, H.; Harada, T.; Kuroda, R.; Bhattacharjee, M. *Inorg. Chem.* **2006**, *45*, 9619−9621.

(10) Constable, E. C. *Prog. Inorg. Chem.* **1994**, *42*, 67−138.

(11) (a) Xiao, D.-R.; Wang, E.-B.; An, H.-Y.; Li, Y.-G.; Xu, L. *Cryst. Growth Des.* **2007**, *7*, 506−512. (b) Enamullah, M.; Sharmin, A.; Hasegawa, M.; Hoshi, T.; Chamayou, A.-C.; Janiak, C. *Eur. J. Inorg. Chem.* **2006**, 2146−2154. (c) Zhang, Y.; Jianmin, L.; Nishiura, M.; Deng, W.; Imamoto, T. *Chem. Lett.* **1999**, 1287−1288. (d) Radford, J. D.; Vittal, J. J.; Wu, D. *Angew. Chem., Int. Ed.* **1998**, *37*, 1114−1116.

(12) (a)Telfer, S. G.; Kuroda, R. *Chem.-Eur. J.* **2005**, *11*, 57−68. (b) Telfer, S. G.; Sato, T.; Kuroda, R. *Angew. Chem., Int. Ed.* **2004**, *43*, 581−584.

(13) (a) Lonnon, D. G.; Colbran, S. B.; Craig, D. C. *Eur. J. Inorg. Chem.* **2006**, 1190−1197. (b) Pradeep, C. P.; Zacharias, P. S.; Das, S. K. *Eur. J. Inorg. Chem.* **2005**, 3405−3408.

(14) (a) Prabhakar, M.; Zacharias, P. S.; Das, S. K. *Inorg. Chem.* **2005**, *44*, 2585−2587. (b) Balamurugan, V.; Hundal, M. S.; Mukherjee, R. *Chem.-Eur. J.* **2004**, *10*, 1683−1690. (c) Balamurugan, V.; Jacob, W.; Mukherjee, J.; Mukherjee, R. *Cryst. Eng. Comm.* **2004**, *6*, 396−400.

(15) (a) McMorran, D. A.; Steel, P. J. *Inorg. Chem. Commun.* **2003**, *6*, 43−47. (b) McMorran, D. A.; Steel, P. J. *Chem. Commun.* **2002**, 2120−2121.

(16) Argent, S. P.; Adams, H.; Riis-Johannessen, T.; Jeffery, J. C.; Harding, L. P.; Clegg, W.; Harrington, R. W.; Ward, M. D. *Dalton Trans.* **2006**, 4996−5013 and references therein.

Scheme 2. Assembly of Chiral Tectons to Give Helical or *meso*-Helical Polymeric Structures

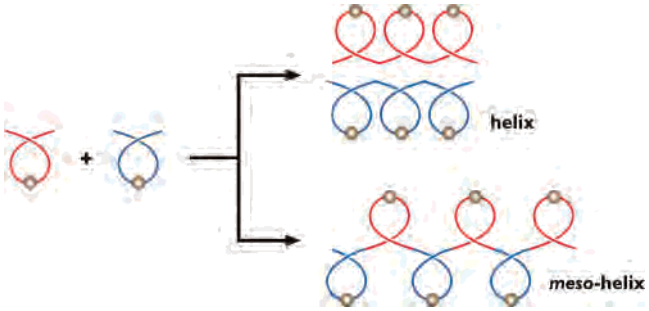

these tectons possess axial chirality due to the way in which the ligands coordinate to the metal ion. In two of the five complexes structurally characterized, 1-dimensional helical chains are found in which Ag**L**$_2$ tectons of the same chirality are hydrogen bonded together, either directly or mediated by anions. The resulting overall structures contain both M (left handed) and P (right handed) helical chains. In the other three structures, Ag**L**$_2$ tectons of alternating chirality are hydrogen bonded together, either directly or mediated by solvent molecules, to give achiral *meso*-helical chains. While the helix (a three-dimensional transformation of a circle) is a very common structural motif in metallosupramolecular chemistry, as discussed above, the *meso*-helix (a three-dimensional transformation of a lemniscate or figure-eight) is very much less common.[17] However, both are equally valid ways of assembling the Ag**L**$_2$ tectons, with, on the one hand, the tectons segregated according to their chirality in the overall structure whereas, on the other, tectons of both chiralities are accommodated into the one structural motif (Scheme 2).

The current examples are, to our knowledge, the first metal-containing *meso*-helical structures to be prepared using hydrogen bonding. A related organic example, the hydrogen-bonded *meso*-helical structure of *m*-phenylene dioxamic acid diethyl ester, has been reported.[18]

Experimental Section

General. The ligand precursors 4-bromomethylbenzoic acid[19] and 3-(2-pyridyl)pyrazole[20] were prepared by published procedures. All other chemicals were purchased commercially and used as received. ^{1}H NMR spectra were recorded on a 300 MHz Varian ^{UNITY}INOVA spectrometer at 298 K, referenced to the internal solvent signal. IR spectra were recorded on a Perkin-Elmer Spectrum BX FT-IR spectrometer using KBr discs. Microanalyses were performed at the Campbell Microanalytical Laboratory at the University of Otago. Mass Spectra were collected on a Bruker micrO-TOF-Q spectrometer.

Caution: *Although no problems were encountered in this work, transition metal perchlorates are potentially explosive. They should be prepared in small amounts and handled with care.*

4-(3-(2-Pyridyl)pyrazol-1-ylmethyl)benzoic acid (L). 4-Bromomethylbenzoic acid (1.00 g, 4.65 mmol) and 3-(2-pyridyl)-pyrazole (675 mg, 4.65 mmol) were refluxed together in a mixture of benzene (15 mL), 40% NaOH(aq) (15 mL) and tetrabutylammonium hydroxide (40% solution, 5 drops) for ca. 18 h. The solution was then cooled, the layers separated, and the aqueous layer washed with ethyl acetate (20 mL). The aqueous layer was acidified to pH 6 with concd HCl and then extracted with ethyl acetate (3 × 20 mL). This organic layer was washed with water (2 × 10 mL) and brine (1 × 10 mL) and dried over $MgSO_4$. Removal of the solvent gave a golden oil which solidified on standing to a pale yellow solid. Recrystallization from hot ethyl acetate/ethanol 1:1 gave a pale yellow crystalline solid. Yield 53%. mp 207−208 °C. Anal. Calcd for $C_{16}H_{13}N_3O_2$: C, 68.81; H, 4.69; N, 15.04. Found: C, 68.98; H, 4.85; N, 15.32. ^{1}H NMR (CD_3OD, 300 MHz) δ 5.54 (s, 2H, CH_2), 6.97 (d, 1H, H_e), 7.37 (m, 1H, H_b), 7.38 (d, 2H, H_g), 7.82 (d, 1H, H_f), 7.90 (td,1H, H_c), 8.01 (m, 1H, H_d), 8.02 (d, 2H, H_h), 8.56 (d, 1H, H_a). Selected IR (KBr, cm^{-1}): ν_{max} 3458 (OH), 1699 (C═O), 1603, 1493, 1272 (C−O).

[Ag(L)$_2$]OTf (1). AgOTf (13.8 mg, 0.054 mmol) was dissolved in methanol (1 mL) and added to **L** (30.0 mg, 0.108 mmol) in methanol (8 mL) to give a clear, pale brown solution. Slow evaporation of the solution gave the product as colorless crystals. Yield 67%. mp >240 °C. Anal. Calcd for $C_{33}H_{26}N_6O_7AgSF_3$: C, 48.60; H, 3.21; N, 10.30. Found: C, 48.72; H, 3.22; N, 10.38. ^{1}H NMR (CD_3OD, 300 MHz): δ 5.26 (s, 2H, CH_2), 7.01 (d, 2H, H_g), 7.09 (d, 1H, H_e), 7.38 (dd, 1H, H_b), 7.56 (d, 2H, H_h), 7.99 (m, 2H, H_c,H_d), 8.09 (d, 1H, H_f), 8.18 (d, 1H, H_a). Selected IR (KBr, cm^{-1}): ν_{max} 3142 (OH), 1727, 1696 (C═O), 1603, 1501, 1296 (C−O), 1223 (OTf^-), 1153 (OTf^-), 1107 (OTf^-), 1025 (OTf^-). Slow evaporation of an acetonitrile/methanol solution of **1** gave a small number of crystals, which were determined by X-ray crystallography to have the composition [Ag**L**$_2$]OTf·1.5H_2O (**1**·1.5H_2O).

[AgL$_2$]NO$_3$ (2·H$_2$O). Complex **2**·H_2O was prepared from $AgNO_3$ as above to give a white crystalline solid. Yield 66%. mp 203−204 °C. Anal. Calc for $C_{32}H_{28}N_7O_8Ag$: C, 51.48; H, 3.78; N, 13.12. Found: C, 51.49; H, 3.66; N, 13.34. ^{1}H NMR (CD_3OD, 300 MHz): δ 5.31 (s, 2H, CH_2), 7.09 (m, 3H, H_e, H_g), 7.40 (dd, 1H, H_h), 7.63 (d, 2H, H_h), 7.98 (m, 2H, H_c, H_d), 8.09 (d, 1H, H_f), 8.24 (d, 1H, H_a). Selected IR (KBr, cm^{-1}): ν_{max} 3447 (OH), 1700 (C═O), 1603, 1492, 1383 (NO_3^-), 1270 (C−O).

[Ag(L)$_2$]PF$_6$ (3·CH$_3$OH). Complex **3**·CH_3OH was prepared as for **1** to give a colorless crystalline solid. Yield 67%. mp 222−225 °C. Anal. Calcd for $C_{33}H_{30}N_6O_5AgPF_6$: C, 46.94; H, 3.58; N, 9.95. Found: C, 47.11; H, 3.48; N, 10.06. ^{1}H NMR (CD_3OD, 300 MHz): δ 5.26 (s, 2H, CH_2), 7.01 (d, 2H, H_g), 7.09 (d, 1H, H_e), 7.38 (dd, 1H, H_b), 7.56 (d, 2H, H_h), 7.99 (m, 2H, H_c,H_d), 8.09 (d, 1H, H_f), 8.19 (d, 1H, H_a). Selected IR (KBr, cm^{-1}): ν_{max} 3448 (OH), 1698 (C═O), 1603, 1493, 1273 (C−O), 847, 560 (PF_6^-). ES-MS (CH_3CN): 667.1105 [Ag**L**$_2$]$^+$, 386.0228 [Ag**L**]$^+$ (100%), 280.1104 [**L**]$^+$.

[Ag(L)$_2$]ClO$_4$ (4·CH$_3$OH). Complex **4**·CH_3OH was prepared as for **1** to give a colorless crystalline solid. Yield 66%. mp > 230 °C. Anal. Calcd for $C_{33}H_{30}N_6O_9AgCl$: C, 49.67; H, 3.79; N, 10.52.

(17) (a) Burchell, T. J.; Puddephatt, R. J. *Inorg. Chem.* **2006**, *45*, 650−659. (c) Luan, X.-J.; Cai, X.- H.; Wang, Y.-Y.; Li, D.-S.; Wang, C.-J.; Liu, P.; Hu, H.-M.; Shi, Q.-Z.; Peng, S.-M. *Chem. Eur. J.* **2006**, *12*, 6281−6289. (d) Son, S. U.; Park, K. H.; Kim, B. Y.; Chung, Y. K. *Cryst. Growth Des.* **2003**, *3*, 507−512. (e) Cai, Y.-P.; Zhang, H.-X.; Xu, A.- W.; u, C.-Y.; Chen, C.-L.; Liu, H.- Q.; Zhang, L.; Kang, B.-S. *J. Chem. Soc. Dalton Trans.* **2001**, 2429−2434. (f) Plasseraud, L.; Maid, H.; Hampel, F.; Saalfrank, R. W. *Chem. Eur. J.* **2001**, *7*, 4007−4011. (g) Ratilainen, J.; Airola, K.; Frölich, R.; Nieger, M.; Rissanen, K. *Polyhedron* **1999**, *18*, 2265−2273. (h) Airola, K.; Ratilainen, J.; Nyrönen, T.; Rissanen, K. *Inorg. Chim. Acta* **1998**, *277*, 55−60.

(18) Blay, G.; Fernández, I.; Pedro, J. R.; Ruiz-García, R.; Carmen Munoz, M.; Cano, J.; Carrasco, R. *Eur. J. Org. Chem.* **2003**, 1627−1630.

(19) Schuster, M. C.; Mann, D. A.; Buchholz, T. J.; Johnson, K. M.; Thomas, W. D.; Kiessling, L. L. *Org. Lett.* **2003**, *5*, 1407−1410.

(20) Amoroso, A. J.; Cargill Thompson, A. M.; Jeffrey, J. C.; Jones, P. L.; McCleverty, J. A.; Ward, M. D. *J. Chem. Soc. Chem. Commun.* **1994**, 2751−2752.

Table 1. Crystal Data for **L** and **1**−**4**·CH_3OH

	L	**1**	**1**·1.5H_2O	**2**	**3**·CH_3OH	**4**·CH_3OH
formula	$C_{16}H_{13}N_3O_2$	$C_{33}H_{26}AgF_3N_6O_7S$	$C_{16.5}H_{15}Ag_{0.5}F_{1.5}N_3O_{4.75}S_{0.5}$	$C_{16}H_{13}Ag_{0.5}N_{3.5}O_{3.5}$	$C_{33}H_{30}AgF_6N_6O_5P$	$C_{33}H_{30}AgClN_6O_9$
fw	279.29	815.53	429.78	364.23	843.47	797.95
cryst syst	orthorhombic	monoclinic	monoclinic	orthorhombic	triclinic	triclinic
a (Å)	7.4682(2)	14.568(3)	19.0056(17)	13.3534(6)	12.1546(7)	11.6894(19)
b (Å)	16.0485(5)	19.028(4)	18.7539(16)	16.6898(8)	13.0571(7)	12.967(2)
c (Å)	22.0992(7)	13.933(3)	13.4069(12)	26.1459(18)	13.4179(8)	13.407(2)
α (deg)	90	90	90	90	72.723(2)	85.429(3)
β (deg)	90	121.002(7)	131.387(3)	90	63.402(2)	64.351(3)
γ (deg)	90	90	90	90	63.561(2)	65.069(3)
V (Å^3)	2648.66(14)	3310.5(11)	3585.2(5)	5827.0(6)	1692.23(17)	1648.1(5)
ρ_{calcd}/g cm^{-1}	1.401	1.636	1.592	1.661	1.655	1.608
space group	*Pbca*	*Cc*	*C*2/*c*	*Fdd*2	$P\bar{1}$	$P\bar{1}$
Z	8	4	8	16	2	2
μ (mm^{-1})	0.095	0.748	0.700	0.756	0.728	0.758
F(000)	1168	1648	1744	2960	852	812
dimens (mm^3)	0.53 × 0.26 × 0.15	0.28 × 0.23 × 0.05	0.40 × 0.20 × 0.10	0.69 × 0.48 × 0.21	0.68 × 0.18 × 0.18	0.35 × 0.20 × 0.09
T (K)	86(2)	89(2)	89(2)	86(2)	86(2)	89(2)
no. measured	82 729	27 969	22 514	39 865	32 312	28 654
data/restraints/ params	4842/0/191	4262/6/460	4300/9/251	5366/1/215	9029/0/476	7428/43/484
GOF on F^2	1.024	1.078	1.064	1.049	1.248	1.045
final *R* indices	R1 = 0.0430	R1 = 0.0472	R1 = 0.0677	R1 = 0.0170	R1 = 0.0306	R1 = 0.0810
[$I > 2\sigma(I)$]	wR2 = 0.1120	wR2 = 0.1135	wR2 = 0.1904	wR2 = 0.0466	wR2 = 0.882	wR2 = 0.2220
R indices	R1 = 0.0538	R1 = 0.0556	R1 = 0.0847	R1 = 0.0172	R1 = 0.0365	R1 = 0.0956
(all data)	wR2 = 0.1215	wR2 = 0.1169	wR2 = 0.2095	wR2 = 0.0468	wR2 = 0.0980	wR2 = 0.2355

Found: C, 49.43; H, 3.65; N, 10.50. ^{1}H NMR (CD_3OD, 300 MHz): δ 5.24 (s, 2H, CH_2), 6.99 (d, 2H, H_g), 7.08 (d, 1H, H_e), 7.36 (dd, 1H, H_b), 7.55 (d, 2H, H_h), 7.98 (m, 2H, H_c,H_d), 8.07 (d, 1H, H_f), 8.17 (d, 1H, H_a). Selected IR (KBr, cm^{-1}): ν_{max} 3462 (OH), 1690 (C═O), 1603, 1500, 1281 (C−O), 1099 (ClO_4^-).

Crystallography. Colorless crystals of **L** were grown by slow evaporation of a methanol solution. Colorless crystals of **1**, **3**·CH_3OH, and **4**·CH_3OH were grown by slow evaporation of a methanol solution of the complex, while crystals of **3** were grown by slow evaporation of an acetonitrile solution. While the crystals of **1** were of relatively poor quality, attempts to solve the structure using the alternative space group *C*2/*c* were unsuccessful. In **1**·1.5H_2O, the triflate anion was disordered about a crystallographic center of inversion and was modeled satisfactorily with 50% contributions from each of the two orientations. Crystals of **4**·CH_3OH were also of poor quality, and while the cation and the methanol solvate molecule were well resolved, the ClO_4^- anion, which was disordered about a crystallographic center of inversion, could not be satisfactorily resolved. The crystal data, data collection, and refinement parameters are listed in Table 1. All measurements were made with a Bruker ApexII diffractometer using graphite-monochromated Mo Kα (λ = 0.71073 Å) radiation. Intensities were corrected for Lorentz and polarization effects[21] and for absorption using SADABS.[22] The structures were solved by direct methods using SHELXS[23] or SIR97,[24] running within the WinGX package,[25] and refined on F^2 using all data by full-matrix least-squares procedures with SHELXL-97.[23] All non-hydrogen atoms were refined with anisotropic displacement parameters. Hydrogen atoms on carbon and COOH oxygen atoms were included in calculated positions with isotropic displacement parameters 1.2 and 1.5 times the isotropic equivalent of their carrier atoms, respectively. Hydrogen atoms on solvent water and methanol molecules were found from the difference map where possible and refined appropriately. Packing diagrams were prepared using Mercury version 1.4.2.[26]

Scheme 3. Synthesis of **L**[a]

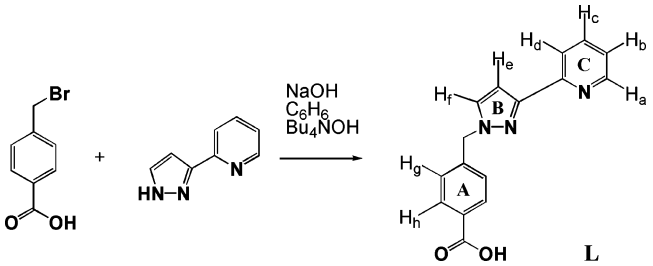

[a] Hydrogen atom labeling (as used in ^{1}H NMR spectral assignment) and ring labeling (as in X-ray structure discussion) are shown.

Results and Discussion

The new ligand **L** was prepared in reasonable yield from 4-bromomethylbenzoic acid and 3-(2-pyridyl)pyrazole by a phase-transfer-catalyzed alkylation reaction (Scheme 3) and was characterized by microanalysis, ^{1}H NMR and infrared spectroscopies, and X-ray crystallography. The IR spectrum showed characteristic peaks for the COOH group at 1699 and 1272 cm^{-1}.[27] The ligand was poorly soluble in most organic solvents but was relatively soluble in methanol.

Ligand **L** was reacted with AgOTf, $AgNO_3$, $AgPF_6$, and $AgClO_4$ in a 1:2 metal/ligand stoichiometry in methanol

(21) (a) *SAINT V4, Area Detector Control and Integration Software;* Siemens Analytical X-ray Systems Inc.: Madison, WI, 1996. (b) Otwinowski, Z.; Minor, W. In *Methods in Enzymology: Macromolecular Crystallography Part A*; Carter, C. W., Jr., Sweet, R. M., Eds.; Academic Press: New York, 1997; Vol. 276, pp 307−326.
(22) Sheldrick, G. M. *SADABS, Program for Absorption Correction*; University of Göttingen: Göttingen, Germany, 1996.
(23) Sheldrick, G. M. *SHELXS and SHELXL*; Institüt für Anorganische Chemie der Universität: Göttingen, Germany, 1996.
(24) Altomare, A.; Burla, M. C.; Camalli, M.; Cascarano, G. L.; Giacovazzo, C.; Guagliardi, A.; Moliterni, A. G. G.; Polidori, G.; Spagna, R. *J. Appl. Crystallogr.* **1999**, *32*, 115−119.
(25) Farrugia, L. J. *J. Appl. Crystallogr.* **1999**, *32*, 837−838.
(26) *Mercury: visualization and analysis of crystal structures*; Macrae, C. F.; Edgington, P. R.; McCabe, P.; Pidcock, E.; Shields, G. P.; Taylor, R.; Towler, M.; van de Streek, J. *J. Appl. Crystallogr.* **2006**, *39*, 453−457.
(27) Nakamoto, M. *Infrared and Raman Spectra of Inorganic and Coordination Compounds, Part B*; Wiley-Interscience: New York, 1997.

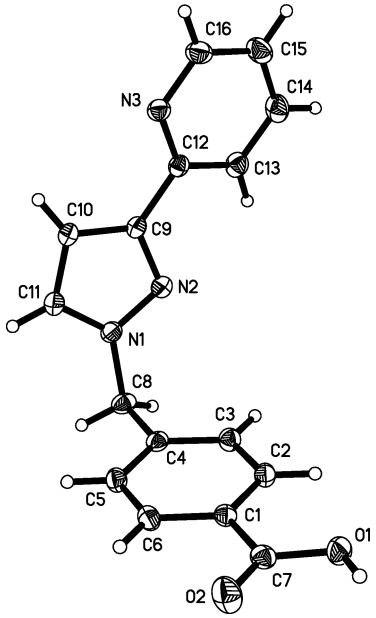

Figure 1. View of the X-ray crystal structure of **L**. Thermal ellipsoids are drawn at the 50% probability level.

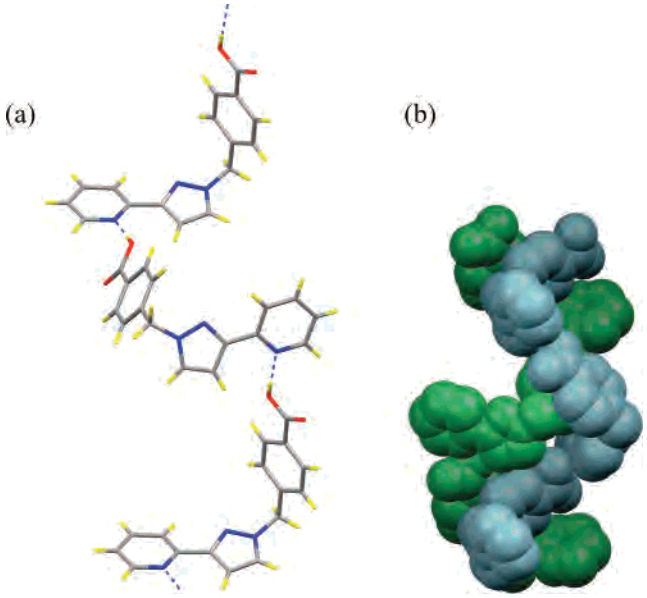

Figure 2. (a) View of one of the helical chains (M helix) formed by **L** in the solid state. (b) View of two adjacent, intertwined helical chains (M helix in blue, P helix in green).

Table 2. Selected Distances (Å) and Angles (deg) for **L** and **1**−**3**·CH_3OH

	L	**1**	**1**·1.5H_2O	**2**	**3**·CH_3OH
		Bond Distances (Å)			
Ag1−N2		2.355(7)	2.358(4)	2.4212(8)	2.4150(12)
Ag1−N3		2.308(8)	2.266(4)	2.2604(8)	2.2535(12)
Ag1−N5		2.379(8)			2.4357(14)
Ag1−N6		2.274(8)			2.2471(12)
		Bond Angles (deg)			
N2−Ag1−N5		112.2(3)			112.47(4)
N2−Ag1−N6		133.5(3)			116.71(4)
N3−Ag1−N5		136.7(3)			115.55(4)
N3−Ag1−N6		138.5(3)			165.22(4)
N2−Ag1−N2A			122.55(18)	114.86(4)	
N2−Ag1−N3A			119.30(15)	109.16(3)	
N3−Ag1−N3A			157.1(2)	176.04(5)	
		Plane Distances (Å)			
A···D			3.54	3.38	3.54
		Plane Angles (deg)			
A−D		85.40	6.86	82.28	8.68
B−C	162.91	12.25	2.45	10.65	3.60
A−C	88.96	83.39	76.11	87.64	83.11
A−F		12.52	70.47	17.99	
C−F		83.88	76.18	82.09	88.03
D−F		87.68			84.29
E−F		8.79			5.25

solutions. In all cases, colorless crystalline solids, **1**, **2**·H_2O, **3**·CH_3OH, and **4**·CH_3OH, were obtained in good yields from slow evaporation of the reaction solvent. Microanalyses confirmed that, in each case, the 2:1 ligand-to-metal ratio was conserved in these complexes. IR spectroscopy showed that the carboxylic acid group was protonated, and so not involved in metal binding, in each case, with peaks at 1727, 1696, and 1296; 1700 and 1270; 1698 and 1273; and 1690 and 1281 cm^{-1} for **1**, **2**·H_2O, **3**·CH_3OH, and **4**·CH_3OH, respectively. The observation of two C═O peaks for **1** (and possibly two C−O peaks, with the second obscured by the OTf^- peaks) suggests two different types of COOH group in the molecule. This is found to be consistent with the X-ray structure of **1** (see Discussion below). ^1H NMR spectra for **1** and **2**−**4** showed similar chemical shifts for each of the peaks of the pyridine and pyrazole rings: the small differences between these and positions of the related peaks in the spectrum of **L** are consistent with expected coordination-induced shifts.[15] Much larger shifts are observed for the protons on benzoic acid rings, ranging between 0.31 and 0.46 ppm upfield compared to free **L**. The number of peaks and the observed peak shifts suggest that a single complex predominates in solution. The observed shifts in the A ring peaks are consistent with these rings being involved in intramolecular $\pi-\pi$ stacking interactions in an Ag$\mathbf{L}_2$ species, with a structure similar to that found for **3**·CH_3OH (see later). ES-MS spectra of **4** in dilute acetonitrile solution show peaks corresponding to Ag$\mathbf{L}_2^+$, Ag$\mathbf{L}^+$, and $\mathbf{L}^+$ species, supporting the suggestion that the complexes maintain their integrity in solution.

The ligand **L** crystallized in the orthorhombic space group *Pbca* with the asymmetric unit containing a single **L** molecule (Figure 1). The nitrogen donor atoms of the chelating region are transoid, as is commonly found in free ligands of this type. The angle between the pyridyl (C) ring and the pyrazolyl (B) ring is 162.91°, while the pyridyl ring and the benzoic acid (A) ring are almost orthogonal with an angle between the rings of 88.96° (Table 2).

Each ligand molecule is associated with two others via hydrogen bonds between the pyridyl ring nitrogen and the OH group of the benzoic acid ring (Figure 2a, Table 3). This type of hydrogen-bond interaction has been shown to be favored over the alternative $R^2_2(8)$[28] COOH dimer.[29] These hydrogen-bonding interactions, which mirror the way in which the ligand is anticipated to behave in the metal complexes (with the nitrogen donors chelating to the metal rather than hydrogen bonding), reveal the molecule to adopt a chiral conformation in the solid state (Scheme 4).[30]

(28) Etter, M. C. *Acc. Chem. Res.* **1990**, *23*, 120−126.
(29) Steiner, T. *Acta Crystallogr., Sect. B* **2001**, *B57*, 103−106.

Table 3. Hydrogen Bond Data[a]

	d(D···A)/Å	∠(D−H···A)/deg
	L	
O(1)−H(1)···N(3)$^{\#1}$	2.6569(10)	171.4
	1	
O(1)−H(1)···O(5)	2.687(9)	160.6
O(3)−H(3)···O(2)$^{\#2}$	2.639(9)	154.0
	1·1.5H_2O	
O(6)-H(6C)···O(2)	2.727(7)	171(10)
O(1)−H(1)···O(6)$^{\#3}$	2.582(7)	165.2
	2	
O(1)−H(1)···O(3)	2.6574(9)	169.8
	3·CH_3OH	
O(1)-H(1B)···O(50)	2.5847(17)	173(2)
O(3)-H(3B)···O(4)$^{\#4}$	2.6282(17)	178(2)
O(50)-H(50A)···O(2)$^{\#5}$	2.7677(18)	170(2)

[a] Symmetry transformations: #1, $-x+1$, $y-1/2$, $-z+1/2$; #2, $x-1/2$, $y+1/2$, $z-1$; #3, $-x+1$, $-y-1$, $-z$; #4, $-x+1$, $-y+1$, $-z+2$; #5, $-x$, $-y+1$, $-z+2$.

Scheme 4. Enantiomeric Forms of **L**, as Found in the Solid State

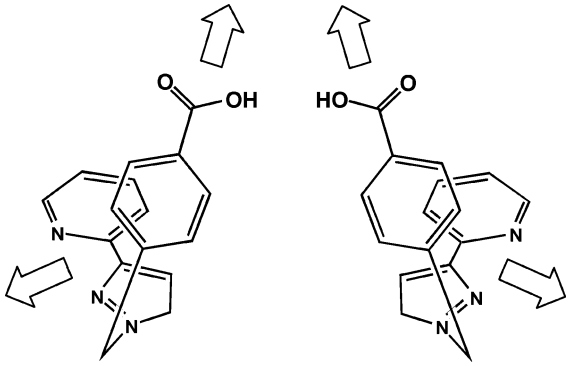

Each ligand molecule forms hydrogen bonds to two others of the same chirality, generating helical chains of ligands which run parallel to the *b* axis, with a helical pitch of 16.049 Å. Consideration of the packing of the one-dimensional helices shows that helices of opposite chirality intertwine. These are held together by strong $\pi-\pi$ stacking interactions, running parallel to the *a* axis, between benzoic acid rings of adjacent chains; the intercentroid distance is 3.76 Å and the angle between the ring planes is 2.33° (Figure 2b).

Slow evaporation of a methanol solution of **1** gave crystals suitable for X-ray analysis. **1** crystallizes in the monoclinic space group *Cc* with the asymmetric unit containing one Ag atom, two coordinated **L** ligands and one triflate anion (Figure 3). The Ag atom is coordinated by the pyridine nitrogens (N_{py}) of each ligand, with Ag−N_{py} distances of 2.274(8) and 2.308(8) Å and also more weakly by the pyrazole nitrogens (N_{pz}), with Ag−N_{pz} distances of 2.355-(7) and 2.379(8) Å. Weaker binding of the pyrazole donors in ligands of this type has been reported previously.[15] Also, the bonding of the pyrazole nitrogens to the Ag atom is significantly out of the pyrazole ring plane, with Ag−N-centroid angles of 163.20° and 164.65°. Again, this has been previously noted.[15] The N_{py}−Ag−N_{py} bond angle is 138.5°, giving a geometry best described as distorted tetrahedral.

(30) Eliel, E. L.; Wilen, S. H.; Mander, L. N. *Stereochemistry of Organic Compounds*; Wiley-Interscience: New York, 1994.

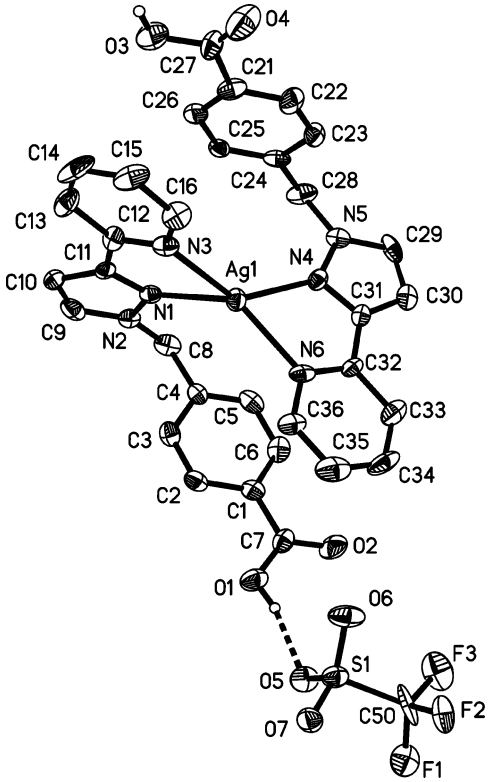

Figure 3. View of the X-ray crystal structure of **1** (Δ configuration). Hydrogen atoms, except those involved in hydrogen bonding interactions, are omitted for clarity. Thermal ellipsoids are drawn at the 30% probability level.

The ligands adopt conformations similar to that observed in the free ligand. The pyridyl and pyrazole rings are approximately coplanar, with B ring−C ring angles of 12.25° and 8.79°. In each case, however, these rings are almost orthogonal to their respective A rings, with A ring−C ring angles of 83.39° and 87.68°. Further, the B ring−C ring planes of each ligand are almost orthogonal to each other, with an angle between the C rings of 83.88° and an angle between the A rings of 85.40°. Stabilizing this orientation of the ligands are intramolecular $\pi-\pi$ stacking interactions between, in each case, the A ring of one ligand and the C ring of the other, with an intercentroid distance of 3.88 Å. The nature of the ligand conformations give the Ag$\mathbf{L}_2$ tecton an axis of chirality, bisecting the N_1−Ag−N_6 and N_3−Ag−N_4 angles.

The triflate forms a hydrogen-bonding interaction to the COOH group of one of the ligands (Table 3, Figure 3). This COOH group also acts as the acceptor in a hydrogen bond to the COOH group on an adjacent Ag$\mathbf{L}_2$ tecton. The COOH group on the other ligand is only involved in an intertecton hydrogen bond. Thus, the structure contains two different types of COOH group, consistent with the IR spectrum of **1**. Each tecton in the chain has the same chirality, so **1** forms one-dimensional helical chains in the crystal, propagating parallel to the intersection of the (−1, 1, 1) and (1, 1, 0) planes (Figure 4a) with a helical pitch of 15.27 Å. Helical chains of the same chirality are arranged in sheets lying in the (2, 0, −1) plane with a closest distance between chains of 8.40 Å. At this distance there can be no interchain interactions by which the helicity of one chain is directed

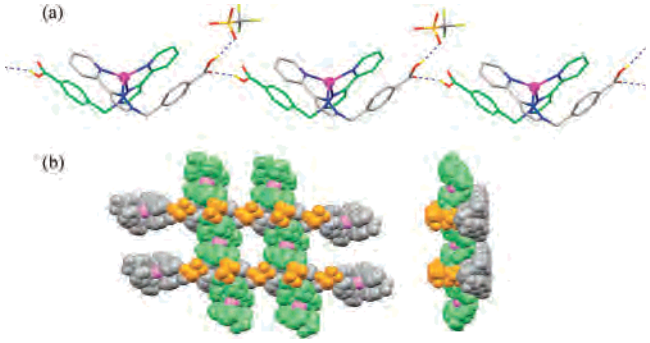

Figure 4. (a) View of one of the 1-dimensional hydrogen-bonded helical chains of **1** (P helix) with ligands colored to emphasize the helical structure. (b) View of the packing of the helical chains of **1** in three dimensions, looking down the *a* axis (left) and perpendicular to the *a* axis (right). Sheets of M helical chains are in green, while the adjacent sheet of P helical chains are in gray. Triflate anions are orange.

by the helicity of its neighbors. The adjacent sheet, which contains helical chains of the opposite chirality, lies parallel to the first but with the chains in the second lying at an angle of 77.1° to those in the first. The second sheet slots into grooves in the first sheet (Figure 4b) with the chains in adjacent sheets being held together by $\pi-\pi$ stacking interactions between A rings in one sheet and B ring−C ring planes in the other, with an intercentroid distance of 3.60 Å. It appears that it is these interactions which direct the respective helicities of the chains. Subsequent sheets are offset such that the apparent channels in the structure do not propagate through the structure.

Slow evaporation of a solution of **1** in methanol and acetonitrile also gave a small number of crystals suitable for X-ray analysis, along with a large amount of amorphous material. One of these was selected for data collection and, surprisingly, a different structure was found to that of **1**, despite the new complex still having a 1:2 Ag/**L** ratio. The new molecule, **1**·1.5H_2O, crystallizes in the monoclinic space group *C*2/*c* with the asymmetric unit containing one **L** ligand, half a silver atom, one and one-half water molecules and half a triflate anion, which is disordered (Figure 5). As was found for **1**, the silver atom in **1**·1.5H_2O is chelated by the ligand, again with the Ag−N_{pz} bond significantly longer than the Ag−N_{py} bond (Table 2). The N_{py}−Ag−N_{py} bond angle is 157.1(2)°, meaning that the structure has a very distorted tetrahedral structure. The ligand adopts the bent conformation observed previously and the angle between the pyridine rings is 76.18° but, in contrast to **1**, the two ligands in **1**·1.5H_2O coordinate to the silver such that their A rings are on the same side of the silver and, in fact, form an intramolecular $\pi-\pi$ stacking interaction with each other, with an intercentroid distance of 3.79 Å. The angle between the OH bonds of the two COOH groups is 73.7°. Again, the way in which the ligands wrap around the silver atom gives the Ag$\mathbf{L}_2$ tecton an axis of chirality.

The COOH group of the ligand is hydrogen bonded to a water molecule, which is, in turn, hydrogen bonded to a second water molecule (Figure 6a, Table 3). This second water molecule is itself hydrogen bonded to the triflate anion. However, due to the disordered nature of the triflate and the fact that the second water molecule only has 50% occupancy,

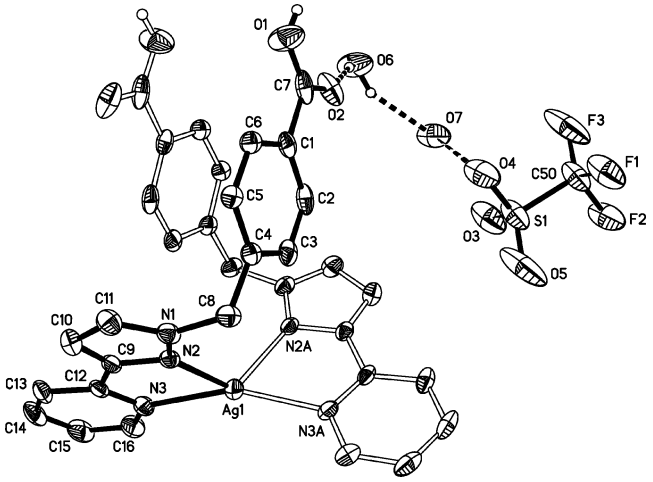

Figure 5. Perspective view of the X-ray crystal structure of **1**·1.5H_2O (Λ configuration). Hydrogen atoms, except those involved in hydrogen-bonding interactions, are omitted for clarity. Only one orientation of the disordered triflate anion is shown. Atoms XA are related to atoms X by the symmetry transformation [$-x+1$, y, $-z+1/2$]. Thermal ellipsoids are drawn at the 30% probability level.

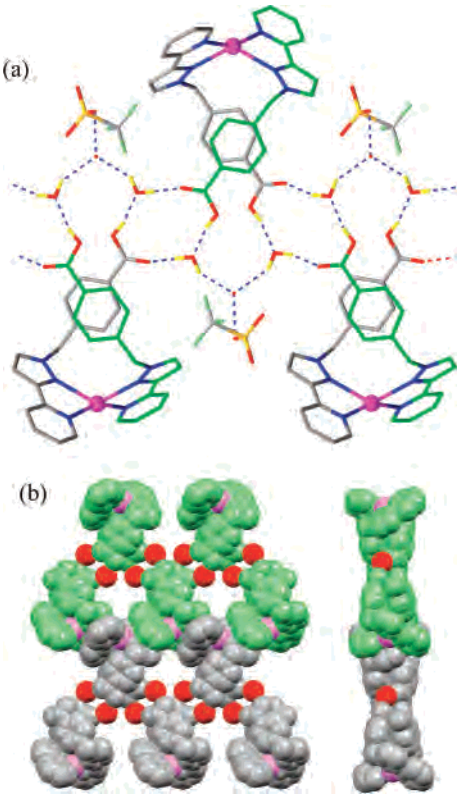

Figure 6. (a) View of one of the one-dimensional hydrogen-bonded *meso*-helical chains of **1**·1.5H_2O with ligands colored to emphasize the *meso*-helical structure. (b) View of the packing of adjacent *meso*-helical chains of **1**·1.5H_2O in three dimensions, looking down the *ac* diagonal (left) and down the *c* axis (right). Full-occupancy water molecules are red. Triflate anions and half-occupancy water molecules are omitted for clarity.

this extended hydrogen-bonding system from the ligand COOH group is only present for half the COOH groups. A second, symmetry-related water molecule also hydrogen bonds to the COOH group and these two then hydrogen bond to the COOH group of a second Ag$\mathbf{L}_2$ unit, giving an R^4_4(12) hydrogen-bonding motif (Figure 6a). This so-called

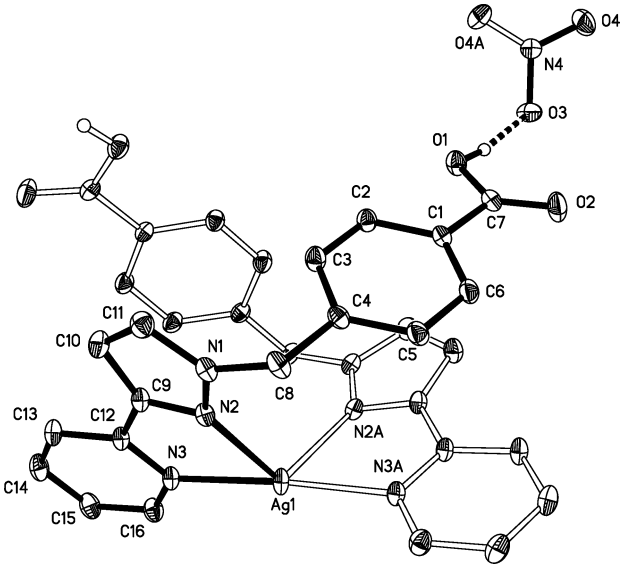

Figure 7. View of the X-ray crystal structure of **2** (Λ configuration). Hydrogen atoms, except those involved in hydrogen-bonding interactions, are omitted for clarity. Atoms XA are related to atoms X by the symmetry transformation [$-x$, $-y$, z]. Thermal ellipsoids are drawn at the 50% probability level.

expanded dimer motif has been reported previously.[31] The second Ag**L**$_2$ tecton is related to the first by a glide reflection and so has opposite chirality to the first. The assembly of Ag**L**$_2$ tectons of alternating Λ and Δ configurations, mediated by the hydrogen-bonded water molecules, generates an infinite one-dimensional *meso*-helical chain which runs parallel to the crystallographic *c* axis. The distance between successive silver atoms in the chain is 18.84 Å, and the pitch of the *meso*-helix is 13.41 Å.

Consideration of the packing shows that the *meso*-helical chains lie in interdigitated sheets parallel to the (2, 0, 0) plane with strong $\pi-\pi$ stacking interactions between the B ring−C ring planes of ligands in adjacent chains (intercentroid distance of 3.68 Å) (Figure 6b). Further, chains in adjacent sheets stack upon each other in such a way as to generate undulating channels, within which the triflate anions and the half-occupancy water molecules reside. These water molecules form bridging hydrogen-bonding interactions between water molecules in adjacent *meso*-helical chains, thereby generating the three-dimensional structure.

Slow evaporation of an acetonitrile solution of **2**·H_2O gave large colorless crystals suitable for X-ray analysis. The complex crystallized in the orthorhombic space group *Fdd*2, with the asymmetric unit containing half an Ag atom, one **L** ligand, and half a nitrate anion (Figure 7). The Ag atom again adopts a distorted tetrahedral geometry (Table 2) with the ligands adopting a bent conformation and the angle between the two pyridyl rings coordinated to the Ag atom being 82.09°. The two ligands wrap around the metal to form a chiral tecton, stabilized by $\pi-\pi$ stacking interactions between the benzoic acid ring of one ligand and the pyridine and pyrazole rings of the other; the angle between the B ring−C ring plane and the A ring of the other ligand is 21.18°

(31) Dunitz, J. D. *Chem. Eur. J.* **1998**, *4*, 745−746.

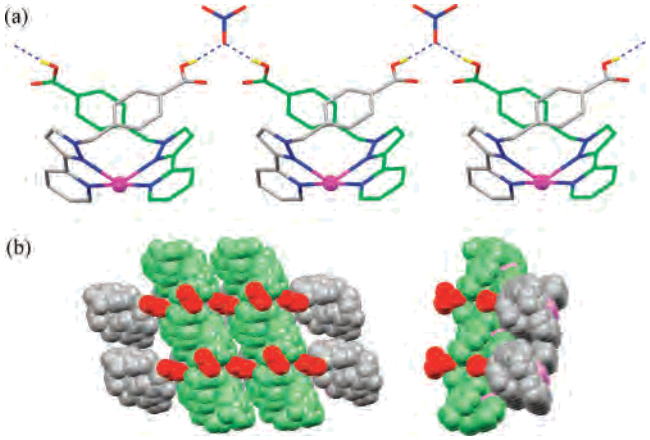

Figure 8. (a) View of one of the one-dimensional hydrogen-bonded helical chains of **2** (M helix) with ligands colored to emphasize the helical structure. (b) View of the packing of the helical chains of **2** in three dimensions, looking down the *c* axis (left) and down the *ab* diagonal (right). Sheets of P helical chains are in green, while the adjacent sheet of M helical chains are in gray. Nitrate anions are red.

and the intercentroid distance is 3.68 Å. The angle between the OH bonds of the two COOH groups is 62.19°.

One of the OH groups hydrogen bonds to the nitrate anion (Table 3) and that same nitrate oxygen atom is further hydrogen bonded to the OH group of a second Ag**L**$_2$. Thus, the bifurcating nitrates assemble identical Ag**L**$_2$ tectons into one-dimensional helical chains, which propagate parallel to the crystallographic *ab* diagonal (Figure 8a). The helical pitch is 10.687 Å. Helical chains of the same chirality form sheets which lie in the (0, 0, 1) plane, with interchain Ag···Ag distances of 10.687 Å. Sheets of helical chains, of alternate chirality, in turn stack upon each other, with the chains in one sheet at 77.3° to those in the next (Figure 8b). The sheets are held together by $\pi-\pi$ stacking interactions between A rings in one chain and C rings in the next: the angle between the rings is 9.21°, and the intercentroid distance is 3.94 Å.

Slow evaporation of methanol solutions of hexafluorophosphate **3** and perchlorate **4** gave colorless crystals. X-ray analysis found the structures of the two compounds to be the same. The following describes the structure of **3**·CH_3OH, but the description equally applies to **4**·CH_3OH. The complex crystallizes as a methanol solvate in the triclinic space group $P\bar{1}$ with the asymmetric unit containing one Ag atom, two **L** ligands, two half PF_6^- anions, and one molecule of methanol (Figure 9). The Ag atom again adopts a distorted tetrahedral geometry (Table 2). The ligand again adopts a bent conformation, with the pyridyl and pyrazolyl rings again approximately coplanar, and these planes approximately orthogonal to the A rings. The angle between the pyridine rings of each ligand is 88.03°, and the two almost parallel A rings form a $\pi-\pi$ stacking interaction, with an intercentroid distance of 3.96 Å. The angle between the OH bonds of the two COOH groups is 77.6°. Again, due to the way that the ligands wrap around the Ag atom, each Ag**L**$_2$ tecton is axially chiral.

In this case, the PF_6^- (or ClO_4^-) anion is not involved in any hydrogen-bonding interactions with the COOH groups of the ligands. Instead, a molecule of methanol is incorporated into an $R^4_4(12)$ hydrogen-bonding motif with COOH

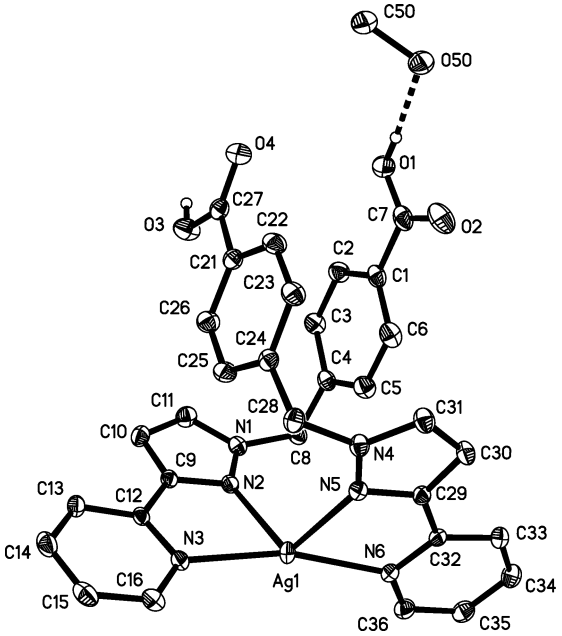

Figure 9. View of the X-ray crystal structure of **3**·CH_3OH (Δ configuration). PF_6^- anions and hydrogen atoms, except those involved in hydrogen-bonding interactions, are omitted for clarity. Thermal ellipsoids are drawn at the 50% probability level.

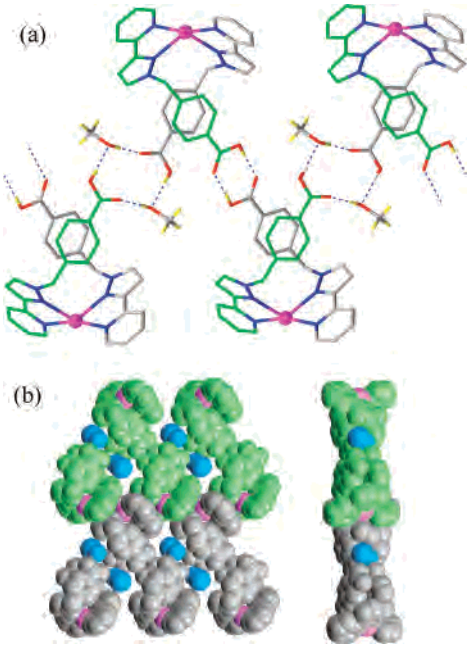

Figure 10. (a) View of one of the one-dimensional hydrogen bonded *meso*-helical chains of **3**·CH_3OH with ligands colored to emphasize the *meso*-helical structure. (b) View of the packing of adjacent *meso*-helical chains of **3**·CH_3OH in three dimensions, viewed in the (0, −1, 1) plane (left) and down the *a* axis (right). Methanol molecules are blue.

groups from adjacent Ag**L**$_2$ tectons, such that pairs of methanol molecules link pairs of Ag**L**$_2$ tectons (Figure 10a, Table 3). This is very similar to the 'extended dimer' motif observed in **1**·1.5H_2O. In this case, however, the second COOH group in each Ag**L**$_2$ unit forms an $R^2_2(8)$ hydrogen bond directly to a COOH group on an adjacent Ag**L**$_2$ unit. Thus, two different types of hydrogen-bonding motif act to link Ag**L**$_2$ tectons of alternating Λ and Δ configurations into *meso*-helical one-dimensional chains, propagating along the

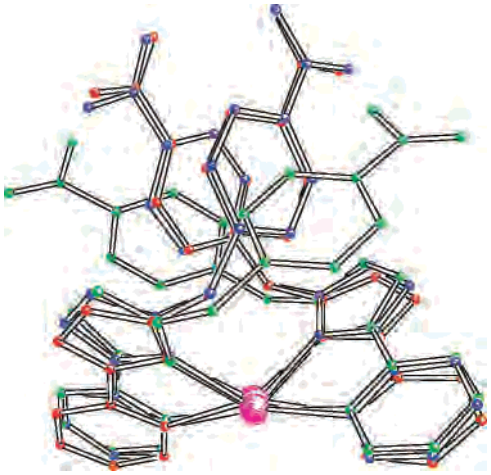

Figure 11. Overlay of the Ag**L**$_2$ tectons of **1**·1.5H_2O (red), **2** (green), and **3**·CH_3OH (blue).

crystallographic *a* axis. The distances between consecutive Ag atoms in the chain are very similar, being 17.925 Å across the $R^4_4(12)$ hydrogen bond and 17.768 Å across the $R^2_2(8)$ hydrogen bond. The pitch of the *meso*-helix is 12.15 Å.

Consideration of the packing in the structure shows that the *meso*-helical chains form sheets which lie in the (0, 2, −2) plane, with adjacent chains interacting via strong $\pi-\pi$ stacking interactions between B ring−C ring planes (Figure 10b). The intercentroid distance is 3.67 Å. These sheets, in turn, stack with chains in adjacent sheets running parallel to each other, again in contrast to **1** and **3**.

Conclusion

The new ligand **L** has been prepared, and complexes formed between it and silver(I) salts have been prepared and structurally characterized. The ligand adopts a chiral conformation in the solid state, which leads it to form one-dimensional helical chains with $OH-N_{py}$ hydrogen bonds joining successive molecules. When chelated to silver, this chiral conformation is maintained and a distorted tetrahedral coordination geometry is observed in all cases. This is in spite of the known plasticity of the Ag(I) coordination geometry. The pyridine nitrogens are more strongly bound than the pyrazole ones; however, the pyrazole donors play a crucial role in the structural nature of the complexes because, by chelating to the silver, the orientation of the hydrogen-bonding synthons (the benzoic acid groups) is more rigorously defined. An overlay of the structures of **1**·1.5H_2O, **2**, and **3**·CH_3OH (Figure 11) shows that there is marked similarity between them, in particular between **1**·1.5H_2O and **3**·CH_3OH (those incorporated into *meso*-helical structures) where, in each case, A ring−A ring $\pi-\pi$ stacking interactions stabilize the structure. **2** is slightly different, due to its adopting A ring−BC ring plane $\pi-\pi$ stacking interactions. Overall, the chelation of the Ag(I), in concert with the intramolecular $\pi-\pi$ stacking interactions, make the Ag**L**$_2$ tecton a more general and reliable structural motif.

^{1}H NMR spectra of the complexes suggest that the tectons are stable in solution and, based on the observed changes in chemical shifts upon coordination of **L**, are likely to adopt

a structure similar to that observed in the X-ray crystal structure of **3**·CH_3OH. This is supported by the ES-MS spectrum of **3**.

The tetrahedral coordination geometry, combined with the bent conformation of the ligands, precludes the formation of discrete [Ag$\mathbf{L}_2$] dimers. Rather, X-ray crystal structures of the silver(I) complexes show that the axially chiral Ag$\mathbf{L}_2$ tectons assemble to form infinite helical or *meso*-helical chains via hydrogen-bonding interactions between the COOH synthon incorporated into **L** and either solvent or anions or, in one case, between the COOH synthons themselves. It has been found that anions can be divided into two types in terms of their hydrogen-bonding nature. So-called spherical anions, such as ClO_4^-, BF_4^-, and PF_6^-, have been found to be poor at hydrogen bonding, whereas nonspherical anions, such as OTf^- and NO_3^-, have been found to be much more readily incorporated into hydrogen bonds.[3f] This is consistent with what has been found in the current study. In **1** and **2**, the anion mediates the hydrogen bonds which join the Ag$\mathbf{L}_2$ tectons into helical chains, whereas in **3**·CH_3OH and **4**·CH_3OH, the anions play no role in the hydrogen-bonding arrays, with solvent molecules instead incorporated. In the case of **1**·$1.5H_2O$, while the OTf^- anions are not involved in the hydrogen bonds forming the *meso*-helical chains, they are involved in the hydrogen-bonding interactions which link adjacent *meso*-helicies.

In two respects, then, the current complexes represent what can be termed reliable tectons for the synthesis of solid-state structures. The chelating nature of the ligands, in combination with the intramolecular $\pi-\pi$ stacking interactions leads, in all cases but one, to the formation of distorted tetrahedral Ag$\mathbf{L}_2$ tectons in which the hydrogen-bonding synthons are in a relatively constant orientation. The hydrogen bonding of these tectons together is then controlled by this orientation and by the nature of the anion chosen; spherical anions lead to *meso*-helical structures in which the anions do not play a role, whereas nonspherical anions generate structures in which they mediate the hydrogen bonding of the tectons into helical chains.

It seems likely that the structural reliability observed in these silver-based tectons might be extended to similar tectons containing other transition metal ions. Such studies on these, and systems with the related ligand 4-(3-(2-pyridyl)-pyrazol-1-ylmethyl)benzoic acid, are under way.

Acknowledgment. Assoc Prof Lyall Hanton is thanked for helpful discussions, and Lisa Bucke is thanked for her assistance in preparing some of the diagrams.

Supporting Information Available: Crystallographic data in CIF format. This material is available free of charge via the Internet at http://pubs.acs.org.

IC701919R